Adsorption 3, 7–25 (1996)

Adsorption of Nitrogen, Methane, Carbon Monoxide, and Their Binary Mixtures on Aluminophosphate Molecular Sieves

L. PREDESCU, F.H. TEZEL AND S. CHOPRA
University of Ottawa, Department of Chemical Engineering, 161 Louis Pasteur, Ottawa, Ontario K1N 6N5, Canada

Abstract. Experimental isotherms describing the adsorption of pure N_2, CH_4 and CO in $AlPO_4$-11, $AlPO_4$-17, and $AlPO_4$-18 were determined using the volumetric method at 40°C and at 23°C ($AlPO_4$-11 only) over a pressure range up to 123 kPa, and subsequently fitted with the Langmuir or Freundlich equations, as well as the Flory-Huggins Vacancy Solution Theory equation. The capacities for the adsorbates investigated were found to depend on the geometry of the sieve pore size, as well as the molecular dimensions and the polarity of the adsorbate involved. At 40°C and over the investigated pressure range, $AlPO_4$-11 and $AlPO_4$-17 adsorbed pure CH_4 in the highest amounts, while $AlPO_4$-18 had a slightly higher capacity for pure CO.

The model parameters obtained by fitting the experimental pure-component isotherms permitted the prediction of binary adsorption information for the CO-N_2, CH_4-CO, and CH_4-N_2 gas mixtures at 101.3 kPa total pressure, using the Extended Langmuir Model, the Ideal Adsorbed Solution Theory, and/or the Flory-Huggins Vacancy Solution Theory for mixtures. An explanation of the behaviour predicted by each model for each adsorption system is attempted.

Keywords: $AlPO_4$ molecular sieves, nitrogen adsorption, methane adsorption, carbon monoxide adsorption, binary adsorption isotherms

1. Introduction

Aluminophosphate molecular sieves are a recent and challenging addition to the adsorption scene, but knowledge of their adsorptive properties is rather scarce in the literature. Even less multicomponent mixture adsorption information is available. Considering the difficulties associated with the experimental determination of binary mixture adsorption isotherms, pure-gas adsorption information becomes vital in the prediction of binary mixture adsorption isotherms and phase equilibria necessary in the design of adsorptive separation units.

The overall objective of this study was to determine the adsorption capacities of aluminophosphate molecular sieves for N_2, CO, and CH_4 at 40°C and pressures up to about 125 kPa, to predict binary mixture adsorption of these gases in aluminophosphate molecular sieves of various pore geometries and dimensions and to improve our understanding of adsorption mechanisms. These gases were chosen for their difference in polarity in order to explain the interactions of non-polar aluminophosphate molecular sieves with a polar molecule like CO, as well as a quadropolar molecule like N_2 and a non-polar molecule like CH_4.

For the prediction of the binary isotherms, the Extended Langmuir Model (Markham and Benton, 1931), the Ideal Adsorbed Solution Theory (Myers and Prausnitz, 1965), and the Flory-Huggins Vacancy Solution Theory for mixtures (Cochran et al., 1985) were applied using the parameters determined from pure-gas isotherms for the three adsorbents, at 101.3 kPa total pressure. In the case of the Ideal Adsorbed Solution Theory, the Langmuir fits for the pure-gas isotherms were used.

Table 1. Structural characteristics of investigated aluminophosphate molecular sieves (Szostak, 1992).

	$AlPO_4$-11	$AlPO_4$-17	$AlPO_4$-18
Chemical composition	$[Al_{20}P_{20}O_{80}]$	$[Al_{18}P_{18}O_{72}]$	$[Al_{24}P_{24}O_{96}]$
Symmetry	Orthorhombic	Hexagonal	Monoclinic
Channel system	Unidimensional	Three-dimensional	Three-dimensional
Ring system	10-member	8-member	8-member
Pore dimensions [Å][1]	3.9 × 6.3	3.6 × 5.1	3.8 × 3.8
Saturation H_2O pore volume[2] [cc/g]	0.16	0.28	0.35

[1]Meier and Olson (1992).
[2]Wilson (1991).

2. Literature Review

Aluminophosphate structures, described in detail by Pluth and Smith (1987), Rudolf and Crowder (1990), Bennett et al. (1986), lack the framework charge balancing cations present in aluminosilicate molecular sieves. Therefore their frameworks feature overall energetic homogeneity. Even though aluminophosphate molecular sieves are considered globally neutral, adsorbate molecules featuring permanent electric moments can interact with a local non-zero framework electric field (Grillet et al., 1994). The stronger interactions existing in smaller-pore aluminophosphate molecular sieves have a greater effect on non-polar molecules like CH_4 than on polar molecules. As the pore size decreases, the short-range dispersive forces become more important than the long-range Coulombic forces. In micropores of size comparable to the size of the adsorbate molecules, the micropore wall exerts an attractive force on the gas molecules which start to fill the micropore volumetrically—a phenomenon similar to capillary condensation that occurs in large pores at high partial pressures (Suzuki, 1990). The adsorbed phase in the micropores is different from the liquid phase resulting from capillary condensation because of the effect of the force field of the pore wall. The adsorption of non-polar molecules in the micropores would have a non-localized character (Grillet et al., 1994). Micropore windows whose apertures are somewhat smaller than the kinetic diameter of the adsorbate molecules can be penetrated as a result of the effects of vibration of both the diffusing molecules and the crystal lattice (Ruthven, 1984).

X-ray powder diffraction and neutron powder diffraction studies indicate that $AlPO_4$-17 is the aluminophosphate structural analogue of erionite (Wilson, 1991). But from the adsorption point of view, only the large cavities with eight-member ring openings of free aperture 3.6 × 5.1 Å in erionite are relevant. $AlPO_4$-18 features monoclinic symmetry like clinoptilolite and chabazite (Szostak, 1992; Simmen et al., 1991), but its novel structure is more closely related to the latter (Lillerud and Akporiaye, 1994). $AlPO_4$-11 features tubular, unidimensional, 10-member ring channels. Table 1 summarizes information related to $AlPO_4$-11, $AlPO_4$-17, and $AlPO_4$-18.

Aluminophosphate molecular sieves like the ten-member ring $AlPO_4$-11 feature permanent dipoles oriented according to the channel direction (Martens and Jacobs, 1994). Because of the lower electronegativity of the Al atom with respect to the P atom, each pair of adjacent Al-P atoms represents a permanent dipole. The polar properties are less pronounced in the eight-member ring aluminophosphate molecular sieves $AlPO_4$-17 and $AlPO_4$-18, because of their three-dimensional channel system which does not allow for the representation of framework as stacked 2-D nets alternately linked by Al and P atoms.

2.1. *Modelling*

2.1.1. Single-Component Adsorption Equilibria. *The Langmuir Isotherm.* This isotherm remains the most useful for data correlation in separation processes based on physical and chemical adsorption (Langmuir, 1918):

$$\theta = \frac{v}{v_m} = \frac{BP}{1 + BP} \tag{1}$$

Although derived for the ideal case of localized adsorption on a uniform surface without lateral

interaction, this isotherm fits experimental data for a surprisingly large number of systems. This performance can be attributed to the fact that large adsorbate molecules tend to average out the effects of heterogeneity on an atomic scale (Graham, 1959). The Langmuir approach assumes that the adsorption system is in dynamic equilibrium and that molecules may adsorb only on a fixed number of well-defined, localized sites which can hold one molecule with no interaction between molecules adsorbed on neighbouring sites, and that the energy of adsorption is constant over all sites.

Freundlich Isotherm. This isotherm was obtained by Zeldowitsh (1935) for physical adsorption on nonuniform surfaces. It is an empirical equation which allows the amount adsorbed to increase indefinitely with pressure:

$$v = kP^{\frac{1}{n}} \tag{2}$$

As is the case with all empirical equations, the parameters have no significant meaning and therefore do not allow extrapolation beyond the range of operating conditions under which they have been determined.

Flory-Huggins Vacancy Solution Theory (FH-VST). This theory is based on the assumption that each of the two phases involved in adsorption (the gas phase and the adsorbed phase) are binary solutions of adsorbate and vacancy, featuring different compositions at equilibrium. As defined by Cochran et al. (1985), the vacancy is an imaginary entity used to quantify the vacuum space which acts as a solvent for the system. Flory-Huggins equation is used to formulate the activity coefficients for the non-ideal solutions that make up the system. The adsorption isotherm is expressed as the equilibrium pressure as a function of the fractional coverage of the molecular sieve upon adsorption:

$$P = \left(\frac{n_1^{\infty}}{b_1}\frac{\theta}{1-\theta}\right)\exp\left(\frac{\alpha_{1v}^2\theta}{1+\alpha_{1v}\theta}\right) \tag{3}$$

where

$\theta = \frac{n_1}{n_1^{\infty}}$ is the fractional coverage of the surface of the molecular sieve
n_1^{∞} is the limiting amount of adsorption
b_1 is the Henry's Law constant
α_{1v} is the gas-solid (adsorbate-vacancy) interaction parameter

This isotherm equation reduces to the Langmuir equation when the gas-solid interaction parameter, α_{1v}, is 0. In that case, the adsorbed phase is considered ideal as there are no interactions between the adsorbate molecules and the vacancy in this phase.

2.1.2. Binary Gas Mixture Adsorption Equilibria. *Extended Langmuir Model (ELM).* This model for multicomponent gas mixture adsorption is based on the same assumptions used for the Langmuir single component isotherm. For a binary mixture adsorption system, the partial pressures of the components in the gas phase, P_1 and P_2, are in equilibrium with fractional coverages θ_1 and θ_2 on the adsorbent surface. The Extended Langmuir Model results from the equality of the rate of adsorption and the rate of desorption at dynamic equilibrium (Markham and Benton, 1931):

$$\theta_1 = \frac{v_1}{v_{m1}} = \frac{B_1P_1}{1 + B_1P_1 + B_2P_2} \tag{4}$$

where v_{m1} is the monolayer amount for component 1 obtained from the single component adsorption data. A similar equation can be written for component 2, as well. This approach is herein termed as "direct-approach ELM" (labelled "d-ELM").

A thermodynamic consistency condition introduced by Broughton (1948) requires that the monolayer adsorption capacities be equal for all the species in the mixture, i.e., $v_{M1} = v_{M2}$ and that the area occupied by each molecular species on the surface of the adsorbent be independent of the area occupied by the other species.

Kemball et al. (1948) acknowledged considerable interaction between adsorbed molecules from the reduction in the area occupied by the adsorbed species when binary mixture adsorption occurs, compared to the area occupied by the adsorbed species when single-component adsorption occurs. To account for the interactions present in the adsorbed phase for binary mixtures, Innes and Rowley (1947) calculated an averaged monolayer volume, $v_M = v_{M1} = v_{M2}$, from the pure-component monolayer volumes (v_{m1}, v_{m2}) and the mole fractions in the adsorbed phase (x_1, x_2):

$$\frac{1}{v_M} = \frac{1}{v_{M1}} = \frac{1}{v_{M2}} = \frac{x_1}{v_{m1}} + \frac{x_2}{v_{m2}} \tag{5}$$

When this averaged monolayer volume is utilized, Eq. (4) becomes:

$$\theta_1 = \frac{v_1}{v_{M1}} = \frac{B_1P_1}{1 + B_1P_1 + B_2P_2} \tag{6}$$

The resulting ELM equation is named in this study as the "averaging-approach ELM" (labelled "a-ELM").

Ideal Adsorbed Solution Theory (IAST). This theory was developed by Myers and Prausnitz (1965) as an adsorption analog of Raoult's Law for vapor-liquid equilibria. It assumes that there are no interactions between adsorbate molecules in the mixture (ideal solution) in the adsorbed phase and that equilibrium is attained at constant temperature when the spreading pressures of the components in the mixture are equal.

If the pure-gas adsorption isotherms on which the IAST predictions are based on are measured for pressure ranges below 101.3 kPa and the difference in polarity of the gaseous species is not too large, then the predictions are very likely to be accurate since at those pressures the assumption of ideal behaviour can be considered valid (Valenzuela and Myers, 1989). This theory would not apply, however, when a binary mixture forms an azeotrope, since the assumption of ideal adsorbed solution is not going to apply.

Flory-Huggins Form of the Vacancy Solution Theory for Mixtures (FH-VST). This theory is acknowledged to be able to predict highly nonideal equilibria such as adsorption azeotropes. It treats gas mixture adsorption as an equilibrium between two vacancy solutions of different compositions. The components of these solutions (adsorbate and vacancy) are characterized by individual activity coefficients to account for the departure from ideal behaviour of the adsorbed phase. The presence of these components in each phase is quantified by mole fractions specific for each phase. The activity coefficients describe the composition dependence of the nonideal solute-solvent (adsorbate-vacancy) interactions and solute-solute (adsorbate-adsorbate) interactions during multicomponent adsorption. Therefore, the further away the activity coefficient is from unity, the more intense these interactions are. The vacancy in the adsorbed phase is described by its own activity coefficient, γ_v, which is a function of the composition of the adsorbed vacancy solution.

The isothermal computational method is described in detail by Cochran et al. (1985). The system of equations is solved by iteration by setting the fugacity coefficients of the components equal to 1 (assumption valid at low pressures), and by selecting the composition of the adsorbed phase (x_i) and the total pressure (101.3 kPa in this study).

Table 2. Synopsis of relevant physical characteristics of the adsorbates investigated.

	N_2	CH_4	CO
Molecular configuration	Linear	Tetrahedral	Linear
Pauling molecular dimensions[1] [Å]	3.0 × 4.1	4.2	3.7 × 4.2
Kinetic diameter[1] [Å]	3.64	3.8	3.76
Formula weight	28	16	28
Normal boiling point [°C]	−195.8	−161.4	−192
Quadrupole moment[2] [$\times 10^{40}$ Cm^2]	−5.0	—	−12.3
Dipole moment[2] [$\times 10^{30}$ Cm]	—	—	0.39
Polarizability [$\times 10^{24}$ cm^3]	1.74	2.593	1.844

[1]Breck (1974).
[2]Grillet et al. (1994).

3. Experimental

The adsorption isotherms were determined using the volumetric method, with the amount adsorbed at each step determined from PVT measurements applied in a mass balance analysis. Prior to each run, approximately one gram of molecular sieve (powder form) was regenerated by heating it in the sample glass flask at 350°C under vacuum (<10 Pa) for a period of minimum 11 hours. Due to the pressure limitations imposed by the pressure transducers on the volumetric adsorption apparatus, isotherms could be determined only for pressure ranges up to 123 kPa.

The adsorbents investigated ($AlPO_4$-11, $AlPO_4$-17, and $AlPO_4$-18) were synthesized and kindly supplied in powder form by Dr. Serge Kaliaguine of Laval University, Ste-Foy, Quebec, Canada. The gases used were nitrogen (min. 99.99%) and methane (99.99%) from Air Products, as well as carbon monoxide and helium (99.995%) from Matheson. Table 2 presents several characteristics of these gases.

Isotherms were determined for the adsorption of N_2, CH_4, and CO at 40°C with $AlPO_4$-11, $AlPO_4$-17, and $AlPO_4$-18, and at 23°C with only $AlPO_4$-11.

4. Results and Discussion

4.1. *Single-Component Adsorption Isotherms*

Langmuir and FH-VST fits were determined for all the pure gas adsorption systems involving $AlPO_4$-11 and $AlPO_4$-18. In the case of $AlPO_4$-17, Freundlich

fit proved to be an excellent alternative when polar CO was involved. The Langmuir equation was unable to fit this experimental isotherm since negative values were obtained for n_m and B_1. Although Langmuir equation could adequately represent the N_2 and CH_4/$AlPO_4$-17 adsorption systems, the Freundlich fits were also determined. Linear regression on Lotus 1-2-3 spreadsheet was used after the linearization of Langmuir and Freundlich isotherms to determine the coefficients for corresponding pure isotherms. For the calculation of the FH-VST parameters, non-linear regression in SAS by using the Marquardt Algorithm was used.

4.1.1. $AlPO_4$-11. The experimental pure-component isotherms of N_2, CH_4, and CO in $AlPO_4$-11 at 23°C and 40°C (Stelmack, 1994) are presented in Fig. 1 along with the corresponding Langmuir and FH-VST fits determined in this study. All six experimental isotherms are favourable, which supports the hypothesis of the relationship between the shape of an isotherm and the steric constrictions encountered by the adsorbate molecule at the micropore aperture: with medium-sized pores like those of $AlPO_4$-11 (3.9 × 6.3 Å), the three adsorbates (molecular dimensions 3.0 × 4.1 Å for N_2, 4.2 Å for CH_4, and 3.7 × 4.2 Å for CO) do not have to overcome steric impediments and the isotherms are therefore favourable. Figure 1 shows that over the investigated pressure range $AlPO_4$-11 features the highest adsorption capacity for CH_4 and the lowest for N_2 with CO being in between. This is an expected result of "equal access" offered by this medium-pore molecular sieve to all gaseous adsorbates of similar molecular dimensions, smaller than those of its pore aperture. CH_4 being the largest molecule is trapped easily within the pores, while N_2 being the smallest molecule can easily leave the adsorbed phase. The capacity for CO accordingly features intermediate values. As expected, the slope of the isotherms as well as the capacities decrease with increasing temperature.

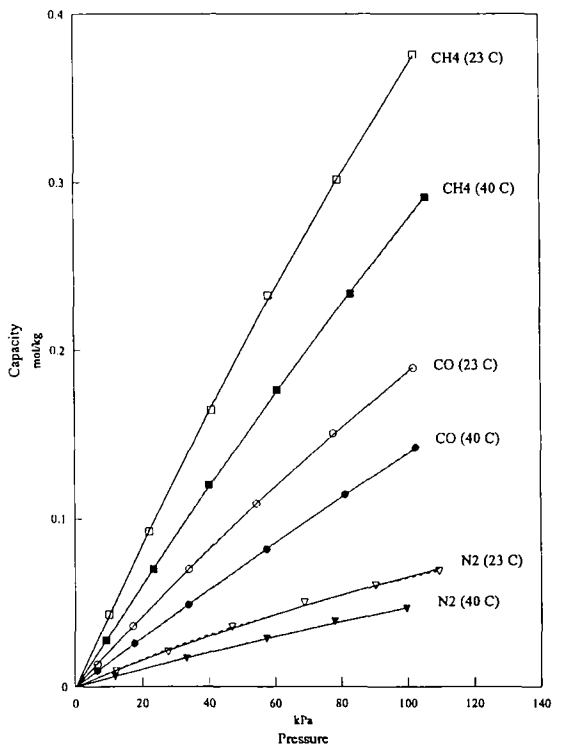

Figure 1. Adsorption of CH_4, N_2, and CO in $AlPO_4$-11 at 23°C and 40°C with corresponding fits: —— Langmuir and - - - - - FH-VST.

All the Langmuir (n_m, B_1) and FH-VST (n_1^{inf}, b_1, α_{1v}) parameters were determined by regression using the experimental data points. These model parameters are valid for the pressure range investigated and are listed in Table 3. With the gas-vacancy interaction parameters (determined from the regression) equal to zero for all six adsorption isotherms, it is not surprising that the Langmuir and the FH-VST fits are excellent and are very similar, since FH-VST reduces to Langmuir at the limit (Henry's Law constant: $b_1 = n_m B_1$, saturation capacity: $n_1^{inf} = n_m$). Difference in parameters come from different approaches to regression which were carried out completely independent from each other. Henry's Law constants are much more closer to each other for these 2 fits than the saturation capacities, since the data are in the range close to the region where this law would apply.

4.1.2. $AlPO_4$-17. The experimental pure-component isotherms of N_2, CH_4, and CO in $AlPO_4$-17 at 40°C are presented in Fig. 2, along with the corresponding FH-VST and Freundlich fits. Langmuir fits for N_2 and CH_4 were carried out, but are not shown in this figure since they would block other fits. This figure shows that at 40°C $AlPO_4$-17 prefers to adsorb CH_4 much more than N_2 and CO in the pressure range studied. The slightly "unfavourable" S-shape observed in the experimental CO/$AlPO_4$-17 and N_2/$AlPO_4$-17 isotherms is due to the steric hindrance encountered by these adsorbate molecules when attempting to penetrate the micropores. $AlPO_4$-17 is a structural analogue of erionite and presents the same "bottle-neck" type of pore geometry,

Table 3. FH-VST (n_1^{inf}, b_1, α_{1v}) and Langmuir (n_m, B_1) parameters for single-component/$AlPO_4$-11 (A11) adsorption isotherms.

Adsorption system	Temperature [°C]	n_1^{inf} [mol/kg]	$b_1 \times 10^6$ [mol/kg Pa]	α_{1v}	n_m [mol/kg]	$B_1 \times 10^6$ [1/Pa]
N_2/A11	40	0.3025	0.56	0	0.3391	1.624
CH_4/A11	40	2.5117	3.113	0	2.7105	1.14
CO/A11	40	2.5765	1.472	0	1.9247	0.776
N_2/A11	23	0.2319	0.903	0	0.29	2.923
CH_4/A11	23	2.304	4.383	0	2.264	1.94
CO/A11	23	1.2702	2.19	0	1.3186	1.652

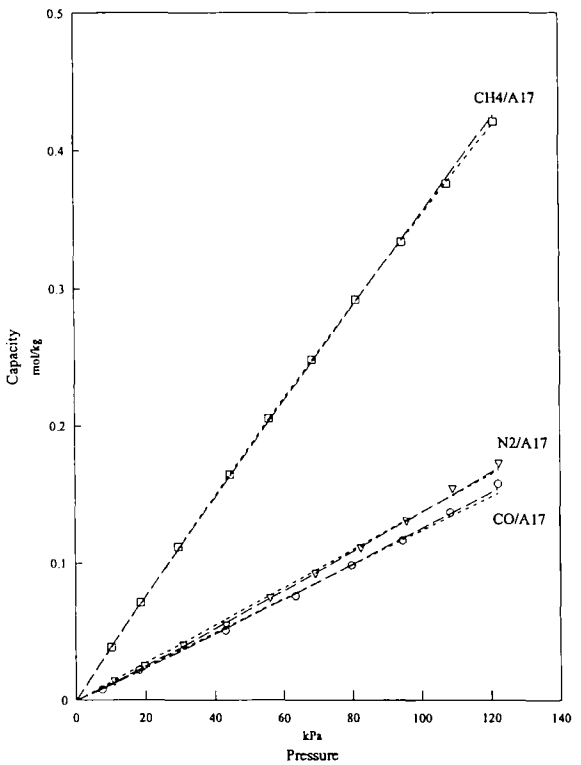

Figure 2. Adsorption of CH_4, N_2, and CO in $AlPO_4$-17 (A17) at 40°C with corresponding fits: – – Freundlich and - - - - - FH-VST.

with elliptical pore apertures which may constitute an impediment for less spherical molecules like N_2 and CO. Steric hindrance is also responsible for the lower capacity for CO. In the case of CH_4 of tetrahedral molecular dimension 4.2 Å (kinetic diameter 3.8 Å), the tetrahedral geometry of the molecules facilitates pore penetration when the molecules approach the opening with one of their four vertices, and then ease themselves as a result of their translational, rotational, and vibrational energies (still present even though reduced upon adsorption on the external surface of the crystal).

The pure CH_4 adsorption isotherm could be correlated with all the isotherm equations with FH-VST equation yielding the best fit. The Langmuir (n_m, B_1), FH-VST (n_1^{inf}, b_1, α_{1v}) and Freundlich (k, n) parameters are listed in Tables 4 and 5. As can be seen from Fig. 2, Freundlich isotherm starts to deviate from the data points at pressures above 90 kPa. Freundlich isotherm fits the N_2 isotherm slightly better than FH-VST. The Langmuir equation was unable to fit the CO experimental isotherm as the linear regression (of P/v vs. P) yielded negative parameters, but the Freundlich equation provided an excellent correlation for this system. Slightly unfavourable shape of CO and N_2 isotherms makes them difficult to fit with Langmuir and FH-VST isotherms.

Several desorption points were also determined on the CO/$AlPO_4$-17 isotherm (Fig. 3), revealing considerable irreversibility of adsorption in the investigated pressure range and the necessity to resort to ultra-high vacuum to desorb most of the CO adsorbed, and ultimately to thermal desorption. The irreversibility curve appears to indicate that once the CO molecules are adsorbed in the micropores, steric considerations concur in impeding desorption when the pressure is reduced. The CO molecules do not have the same translational, rotational, and vibrational freedom (energy) in the micropore cavity, and therefore cannot orient themselves in the position that would permit them to exit the micropore and return to the gas phase above the external surface of the $AlPO_4$-17 crystals, no matter how high the vacuum is.

4.1.3. $AlPO_4$-18. The experimental pure-component isotherms of N_2, CH_4, and CO in $AlPO_4$-18 at 40°C are presented in Fig. 4, along with the corresponding

Table 4. FH-VST (n_1^{inf}, b_1, α_{1v}) and Langmuir (n_m, B_1) parameters for single-component/$AlPO_4$-17 (A17) adsorption isotherms at 40°C.

Adsorption system	Temperature [°C]	n_1^{inf} [mol/kg]	$b_1 \times 10^6$ [mol/kg Pa]	$\alpha_{1v} \times 10^6$	n_m [mol/kg]	$B_1 \times 10^6$ [1/Pa]
N_2/A17	40	1.2682	1.531	4.436	2.6771	0.482
CH_4/A17	40	4.1226	3.853	0	3.877	0.999
CO/A17	40	0.6675	1.563	−4.58	n/a	n/a

Table 5. Freundlich parameters for single-component/$AlPO_4$-17 adsorption isotherms at 40°C.

Adsorbate	Temperature [°C]	k [mol/kg $Pa^{1/n}$]	n
N_2	40	7.0×10^{-7}	0.949
CH_4	40	5.7×10^{-6}	1.044
CO	40	7.8×10^{-7}	0.961

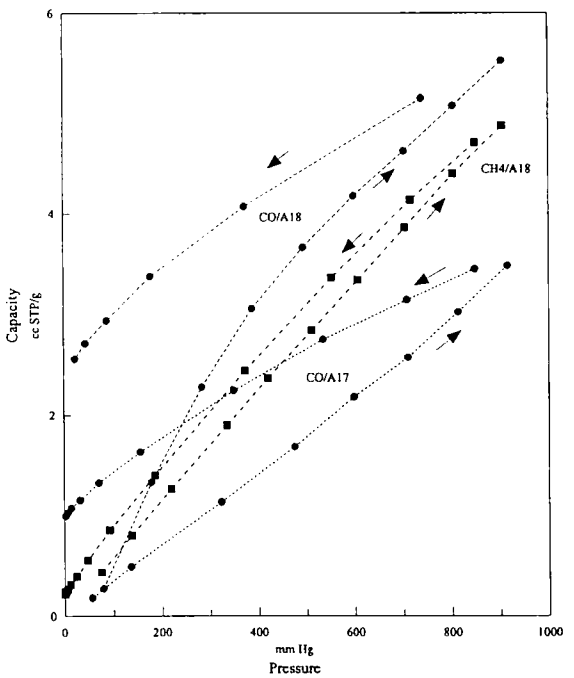

Figure 3. Irreversibility in small-pore aluminophosphate molecular sieves at 40°C as evidence of steric hindrance.

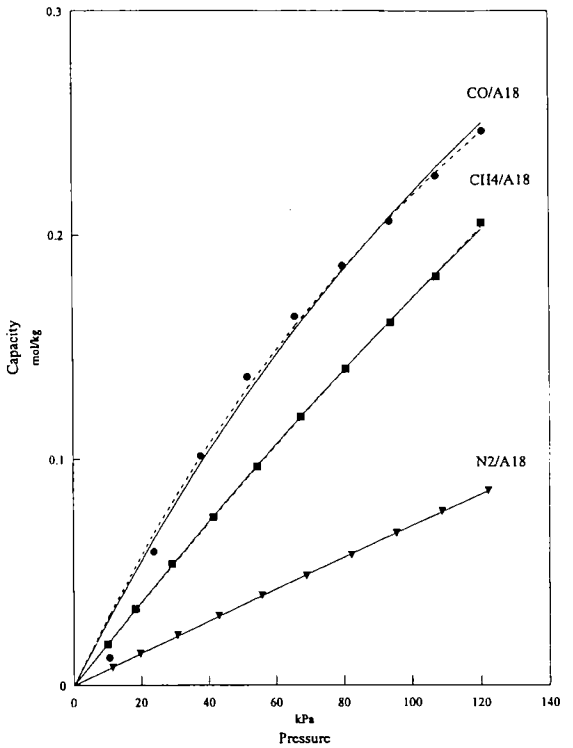

Figure 4. Adsorption of CH_4, N_2, and CO in $AlPO_4$-18 (A18) at 40°C with corresponding fits: —— Langmuir and - - - - - FH-VST.

Langmuir and FH-VST fits. The Langmuir (n_m, B_1) and FH-VST (n_1^{inf}, b_1, α_{1v}) parameters are provided in Table 6. The capacity of $AlPO_4$-18 for the three adsorbates investigated decreases in the order CO > CH_4 ≫ N_2, with the N_2 and CH_4 isotherms featuring obvious linearity within the pressure range studied. The capacity hierarchy could be explained in terms of steric hindrance effects, given the circular pore openings of $AlPO_4$-18 (3.8 × 3.8 Å) and the molecular dimensions of each adsorbate (Table 2).

N_2 is adsorbed in the smallest amounts by $AlPO_4$-18 because of two reasons. Firstly, the larger dimension of the "capsular" N_2 molecule (3.0 × 4.1 Å) cannot fit easily into a circular pore aperture of slightly smaller diameter. Molecular sieves with circular pore apertures are less accessible to "nonspherical" molecules like N_2 or tetrahedral molecules like CH_4 (4.2 Å). Secondly, the weak quadrupole moment in the N_2 molecules is unable to induce electric moments in the atoms on the

Table 6. FH-VST ($n_1^{inf}, b_1, \alpha_{1v}$) and Langmuir ($n_m, B_1$) parameters for single-component/$AlPO_4$-18 (A18) adsorption isotherms at 40°C.

Adsorption system	Temperature [°C]	n_1^{inf} [mol/kg]	$b_1 \times 10^6$ [mol/kg Pa]	α_{1v}	n_m [mol/kg]	$B_1 \times 10^6$ [1/Pa]
N_2/A18	40	4.0747	0.717	0	3.3478	0.215
CH_4/A18	40	2.4393	1.843	0	1.9684	0.952
CO/A18	40	0.7093	3.125	0	0.839	3.517

surface of the adsorbent, but can generate close-range repulsions between neighbouring adsorbed molecules.

CH_4 is more easily accommodated than N_2 since the lack of polarity of the CH_4 molecule prevents the generation of close-range repulsions in the adsorbed phase. The smaller adsorption capacity range of $AlPO_4$-18 for CH_4 with respect to CO is due to the higher kinetic diameter of CH_4 (3.8 Å) being equal to the diameter of the pore opening.

The slightly unfavourable S-shape of the CO isotherm up to 25 kPa could be interpreted as the result of the conjugated effect of energetic interactions and steric factors. Although the kinetic diameter of the CO molecule is 3.76 Å (lower than the diameter of the $AlPO_4$-18 pore aperture), the molecular dimensions are 3.7×4.2 Å. It appears that at low pressure when the concentration of CO molecules in the gas phase is small, the first few molecules end up in the adsorbed phase as a result of the non-specific (adsorbent-related) interactions. The pressure being so low, the first molecules adsorbed in the micropores are probably those which, after being initially adsorbed on the external surface of the crystal, diffuse toward and through the pore openings drawn by the non-specific (adsorbent-related) adsorption potential, and happen to have the adequate orientation necessary to enter the micropore cavity, i.e., they approached the pore window with their smaller molecular dimension (3.7 Å).

The unfavourable part of the CO isotherm in the very low pressure region appears to enforce the idea that pressure was insufficient to help a large number of CO molecules get adsorbed on the external surface of the $AlPO_4$-18 crystals and then diffuse with the appropriate orientation toward and through the pore apertures. Given the energetic homogeneity of the adsorbent, the adsorption potential of the system is also too low at those low pressures. The self-potential contribution paid by only a small number of molecules adsorbed is insufficient to enhance the overall adsorption potential of the system. As soon as some more CO molecules are adsorbed, the self-potential component increases and continues to do so with further adsorption of additional CO molecules.

The adsorbed CO molecules induce "mirror" dipole and quadrupole moments in the framework atoms in the vicinity of which they are lying, thus polarizing the surface of the adsorbent. These electric moments can be more easily induced in the case of this adsorption system because of the close values of the kinetic diameter of the adsorbate and the pore aperture diameter of the adsorbent. As pressure is increased, the concentration of CO in the gas phase above the surface of the adsorbent increases, and the interactions between these gaseous molecules and the polarized adsorbent surface (which now features "self-made" adsorption sites) intensify.

The number of molecular collisions in the gas phase above the crystal also increases with increasing pressure, thus increasing the probability that the molecules in the vicinity of the pore openings have the proper orientation permitting diffusion into the micropore cavities. There appears to be a "threshold" pressure at which the self-potential has reached a value corresponding to a sufficiently polarized surface for the non-polar aluminophosphate molecular material to start behaving like a polar adsorbent with higher potential sites analogous to the cationic sites in zeolites. Above that pressure the slope of the isotherm increases abruptly only to start decreasing the way any favourable type I isotherm flattens when the saturation capacity is approached and close-range repulsions between adsorbed molecules become dominant.

N_2 and CH_4 isotherms were easy to fit with Langmuir and FH-VST equations since they behaved linearly within the pressure range studied. This was not the case for the CO isotherm. Since its shape was slightly unfavourable, these models' interpretation was not as good as the N_2 and CH_4 isotherms, as can be seen from Fig. 4.

Several desorption points were also determined on CH_4/$AlPO_4$-18 and CO/$AlPO_4$-18 isotherms (Fig. 3), revealing that the hysteresis effect is quite important

in the investigated pressure range. Again, the presence of this effect can be explained in terms of steric factors: the adsorbed molecules (whether CH_4 or CO) cannot translate, rotate, and vibrate within the micropores in order to orient themselves in the position that would allow them to leave the micropores and the adsorbed phase in favour of the gas phase around the $AlPO_4$-18 crystals. During desorption, steric hindrance cannot be overcome by a gradient of pressure (as in pressure-swing adsorption system). The solution to this problem would be the incorporation of a thermal-swing desorption, in which case the amplitude and frequency of vibration of the framework increases allowing the adsorbed molecules to exit the micropores at higher temperatures.

4.1.4. Summary. In the absence of adsorbent energetic heterogeneity, adsorption of pure N_2, CO, and CH_4 into aluminophosphate molecular sieves is governed by steric effects. In these systems, the gradient of chemical potential is very small because of the absence of cations, and the success of the adsorption process relies, almost exclusively, on the concentration gradient even at the lowest pressures. Volume filling becomes the predominant mechanism of sorption at high pressures in the gas phase, which permit a large number of molecules to "squeeze" in the micropores.

As far as adsorption capacities are concerned, $AlPO_4$-11 and $AlPO_4$-17 adsorb CH_4 in the highest amounts in the pressure range investigated, while $AlPO_4$-18 prefers to accommodate CO in higher amounts. The smaller molecular dimensions of N_2 are responsible for the inability of $AlPO_4$-11 and $AlPO_4$-18 to retain it in large amounts. These results indicate that steric factors are of tremendous importance in gas adsorption in aluminophosphate molecular sieves.

The adsorption capacities of aluminophosphate molecular sieves are influenced by the nature of the adsorbate. Non-polar and larger molecules would be preferentially adsorbed since the lack of repulsive interactions at high pore fillings enable neighbouring molecules to tolerate the proximity of their peers, and their larger molecular dimensions allow them to be more easily entrapped within the pores. Polar and smaller molecules would be adsorbed in the lowest amounts because of the intense repulsive interactions which are likely to appear at high pore fillings and the smaller molecular dimensions which allow them to readily exit the micropores and return to the gas phase.

Steric factors (pore dimensions and geometry, as well as adsorbate molecular dimensions and geometry) are also responsible for the presence of hysteresis occurring in single-component adsorption in small-pore aluminophosphate molecular sieves. The larger the difference between the micropore aperture diameter and the dimensions of the gas molecule, the less likely is hysteresis in an adsorption system. If steric factors are not favourable (similar pore size and molecular dimensions, and different pore and molecule geometries), the adsorbed molecules are not likely to leave the micropores easily when the pressure is reduced during desorption. Strong hysteresis in an adsorption system makes pressure-swing desorption inefficient and therefore requires incorporation of temperature swing to enhance desorption.

Table 7 summarizes steric accessibility granted by each aluminophosphate molecular sieve to each adsorbate studied.

Confirmation of the reliability of each theory as far as pure gas adsorption modelling is concerned would involve determination of experimental data in the higher superatmospheric pressure range.

4.2. Predicted Binary Mixture Adsorption Isotherms

All predictions have been determined for a total pressure of 101.3 kPa. ELM predictions can be obtained

Table 7. Extent of steric accessibility for the adsorption of N_2, CO, CH_4 in $AlPO_4$-11, $AlPO_4$-17, and $AlPO_4$-18.

Adsorbate	$AlPO_4$-11 ($CH_4 > CO > N_2$)	$AlPO_4$-17 ($CH_4 \gg N_2 > CO$)	$AlPO_4$-18 ($CO > CH_4 \gg N_2$)
N_2	Full	High	Very high
CO	Full	Low[1]	High[2]
CH_4	Full	Very high	Medium[1]

[1]Molecular sieving effect.
[2]Especially at higher pressures.

using two different equations: (i) the "direct-approach" (d-ELM) equation developed by Markham and Benton (1931) and calculating the capacity of the adsorbent for each component in the mixture from the Langmuir monolayer capacities of the pure components, or (ii) the "averaging-approach" (a-ELM) equation resulting from the amendment of the d-ELM equation with the thermodynamic consistency equation developed by Broughton (1948) and used by Innes and Rowley (1947) as well as Innes et al. (1951).

With the linear trend of most of the experimental single-component adsorption isotherms in the pressure range investigated, prediction of binary mixture adsorption must be looked upon with caution. For those aluminophosphate molecular sieves for which pure-gas adsorption data could be correlated by both the Langmuir equation and the FH-VST equation, (that is $AlPO_4$-11 and $AlPO_4$-18), all three models (ELM, IAST, FH-VST) were used to obtain binary mixture adsorption information. For the $AlPO_4$-17 binary mixture adsorption systems, only FH-VST predictions were determined because no reasonable fit could be obtained with the Langmuir equation for the single-component CO isotherm, which is well represented by the Freundlich equation.

Predicted equilibrium separation factors for all the binary systems studied are given in Table 8.

4.2.1. $AlPO_4$-11.

Carbon Monoxide-Nitrogen/$AlPO_4$-11. Figures 5 and 6 show that the models do not agree upon the adsorptive behaviour of this system when compared to each other, but do forecast for each system similar behaviour at different temperatures. IAST and d-ELM predictions are very similar and estimate that the separation would be feasible through preferential adsorption of CO, while a-ELM predicts the preferential adsorption of N_2. The FH-VST predicts an azeotrope formation at 40°C for high CO partial pressures in the gas phase.

Methane-Carbon Monoxide/$AlPO_4$-11. Figures 7 and 8 show that IAST, FH-VST, and d-ELM virtually agree in their predictions, according to which the separation of CH_4 from this mixture using $AlPO_4$-11 would be slightly more successful at 40°C. The a-ELM predicted selectivities are the most conservative, probably as a result of the averaging effect. The predicted selectivity ranges are closer to each other for different models at 23°C than at 40°C (Table 8).

Methane-Nitrogen/$AlPO_4$-11. Figures 9 and 10 show that FH-VST calculations yield a very asymmetric X-Y diagram (which indicates that the values of the separation factors can become huge at very low partial pressures of CH_4). Given the much larger capacity of

Table 8. Predicted equilibrium separation factors for $AlPO_4$-11 (A11), $AlPO_4$-17 (A17), and $AlPO_4$-18 (A18) at 101.3 kPa total pressure for all the adsorption systems.

Binary gas mixture adsorption system	Temperature [°C]	Predicted equilibrium separation factors			
		a-ELM	d-ELM	IAST	FH-VST
CO-N_2/A11	40	0.48	2.71	2.89–3.23	600.2–0.84*
	23	0.57	2.57	2.09–2.12	66.4–1.17
CH_4-CO/A11	40	1.47	2.07	4.51–5.68	2.113–2.111
	23	1.17	2.02	2.09–2.15	2.49–1.80
CH_4-N_2/A11	40	0.70	5.61	6.01–7.97	1065–1.86
	23	0.66	5.18	5.82–9.48	6779–1.44
N_2-CO/A17	40	n/a	n/a	n/a	1.28–0.85*
CH_4-CO/A17	40	n/a	n/a	n/a	121.01–0.96*
CH_4-N_2/A17	40	n/a	n/a	n/a	8.34–1.69
CO-N_2/A18	40	16.36	4.10	3.97–3.69	91.99–0.0007*
CO-CH_4/A18	40	3.70	1.57	1.48–1.44	21.08–0.0004*
CH_4-N_2/A18	40	4.43	2.60	2.58–2.56	2.86–2.25

*Azeotrope.

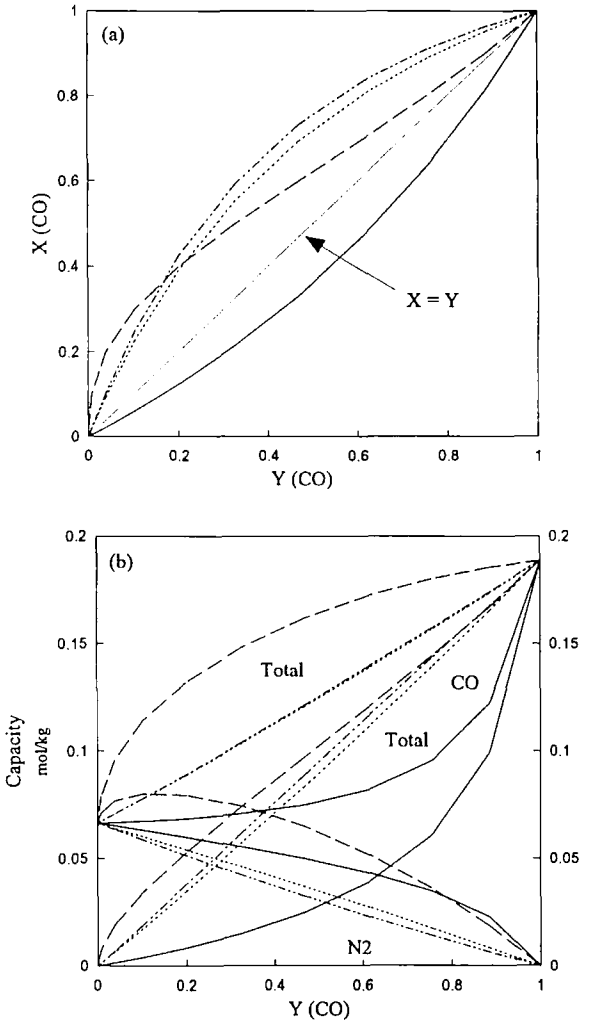

Figure 5. Predicted (a) X-Y diagram and (b) binary equilibrium isotherms for CO-N_2 adsorption in $AlPO_4$-11 at 23°C and 101.3 kPa total pressure: —— a-ELM, - - - - d-ELM, — - - IAST, and — — — FH-VST.

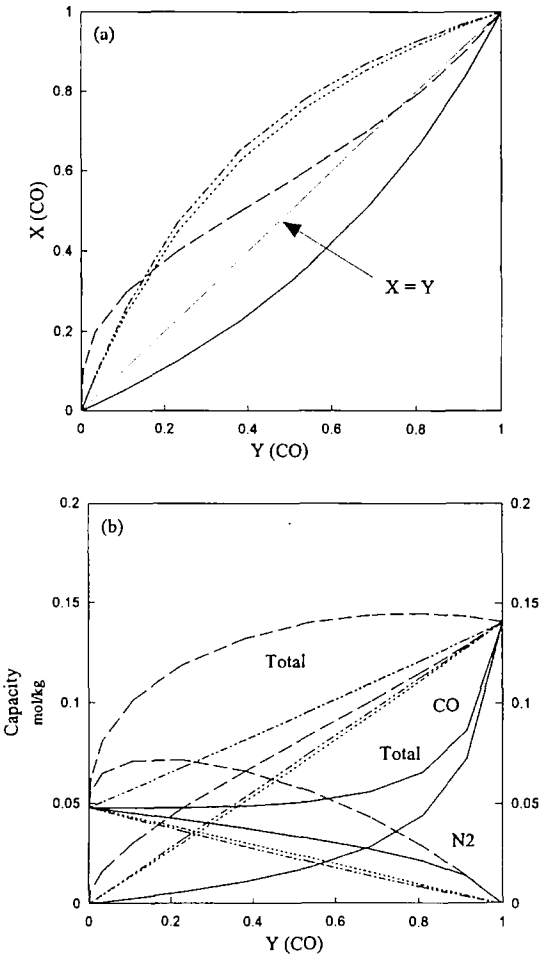

Figure 6. Predicted (a) X-Y diagram and (b) binary equilibrium isotherms for CO-N_2 adsorption in $AlPO_4$-11 at 40°C and 101.3 kPa total pressure: —— a-ELM, - - - - d-ELM, — - - IAST, and — — — FH-VST.

$AlPO_4$-11 for pure CH_4 than for N_2 at 101.3 kPa, the preferential adsorption of CH_4 indicated by IAST, FH-VST, and d-ELM looks reasonable. As expected, the X-Y diagrams yielded by IAST and d-ELM are much more symmetric, predicting similar selectivity values, and the shape of the respective binary isotherms indicates no interactions in the system. At both temperatures, a-ELM predicts the preferential adsorption of N_2, undoubtedly the consequence of averaging.

Summary for $AlPO_4$-11. The diversity of predictions yielded by each model in the case of binary mixture adsorption in $AlPO_4$-11 makes comprehensive interpretation a difficult task. In Table 8, the range-end selectivity values are given for the lowest mole fraction of the reference species (quoted first in the pair) and the highest mole fraction of the reference species for which FH-VST calculations were performed.

Theoretical considerations would indicate that steric effects are not likely to be exerted on the adsorbate molecules seeking access to this medium-pore molecular sieve. Even though the pore apertures are elliptical, since the smaller dimension is larger than the adsorbate molecule with the largest kinetic diameter, CH_4, equal accessibility is offered to both components in all of the three mixtures. The fact that all models agree that CH_4 is preferentially adsorbed from its mixtures

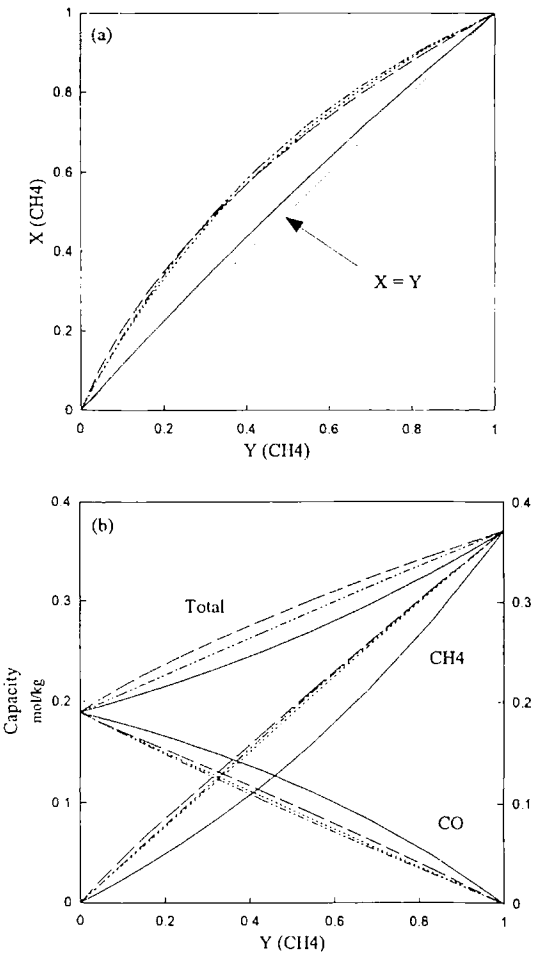

Figure 7. Predicted (a) X-Y diagram and (b) binary equilibrium isotherms for CO-CH_4 adsorption in $AlPO_4$-11 at 23°C and 101.3 kPa total pressure: —— a-ELM, - - - - d-ELM, — - - IAST, and — — — FH-VST.

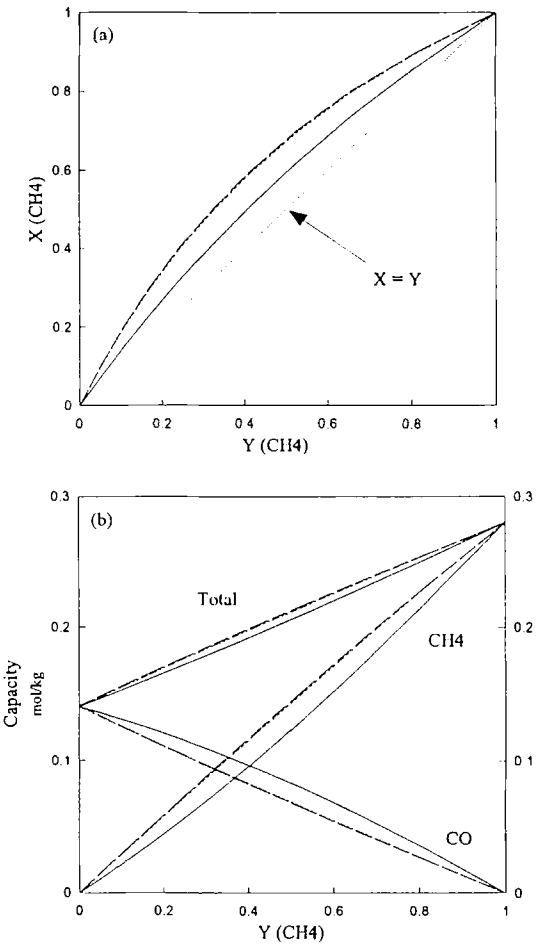

Figure 8. Predicted (a) X-Y diagram and (b) binary equilibrium isotherms for CO-CH_4 adsorption in $AlPO_4$-11 at 40°C and 101.3 kPa total pressure: —— a-ELM, - - - - d-ELM, — - - IAST, and — — — FH-VST.

with CO or N_2 supports the conclusion that this energetically homogeneous molecular sieve accommodates bulkier non-polar molecules like CH_4 in larger amounts since they present a clear advantage with the absence of close-range repulsions in the adsorbed phase. The molecular-dimension criterion also applies in the case of CO-N_2 mixtures, from which $AlPO_4$-11 preferentially retains the larger molecule (CO), which also has the greatest ability to contribute the self-potential much needed by energetically homogeneous adsorbents.

4.2.2. $AlPO_4$-17. FH-VST predictions for binary isotherms of N_2, CO, and CH_4 in $AlPO_4$-17 at 40°C were carried out. As the pure CO experimental equilibrium isotherms could not be fitted with the Langmuir equation, no ELM and IAST predictions were determined for the adsorption of the binary gas mixtures investigated in $AlPO_4$-17 at 40°C.

Nitrogen-Carbon Monoxide/$AlPO_4$-17. According to FH-VST, it would be impossible to separate N_2-CO gas mixtures at 40°C using $AlPO_4$-17 (Fig. 11) because the selectivity values are around unity and because of the anticipated azeotrope. These phenomena should not be surprising considering the similarly low adsorption capacities of $AlPO_4$-17 for pure N_2 and pure CO at 40°C and 101.3 kPa (Fig. 2). Furthermore, both gaseous species must overcome sterically unfavourable geometric factors in order to get adsorbed, with CO being more affected.

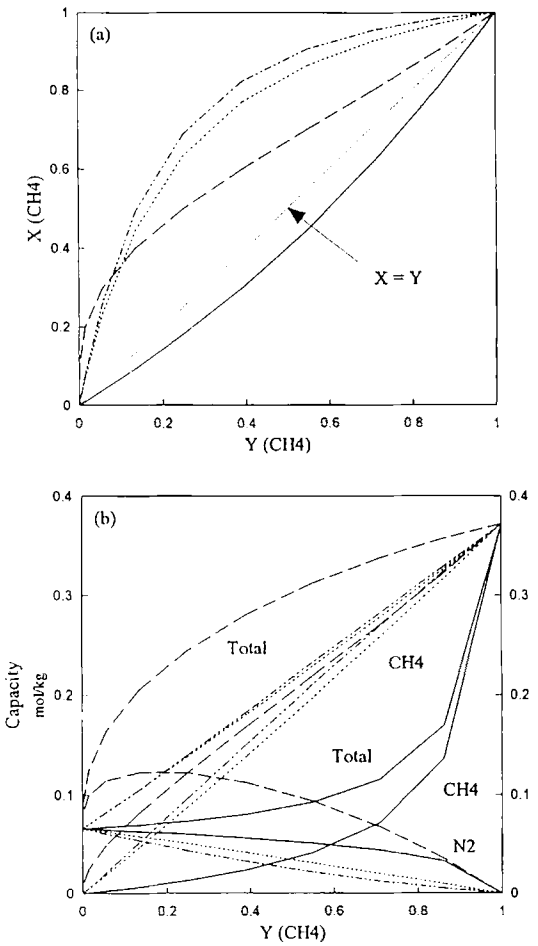

Figure 9. Predicted (a) X-Y diagram and (b) binary equilibrium isotherms for CH_4-N_2 adsorption in $AlPO_4$-11 at 23°C and 101.3 kPa total pressure: — a-ELM, - - - - d-ELM, — - - IAST, and — — — FH-VST.

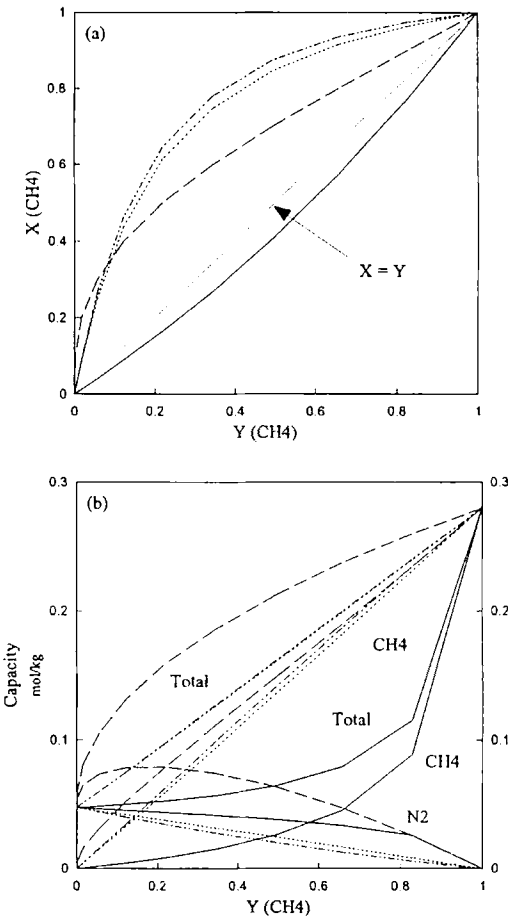

Figure 10. Predicted (a) X-Y diagram and (b) binary equilibrium isotherms for CH_4-N_2 adsorption in $AlPO_4$-11 at 40°C and 101.3 kPa total pressure: — a-ELM, - - - - d-ELM, — - - IAST, and — — — FH-VST.

Methane-Carbon Monoxide/$AlPO_4$-17. Figure 12 reveals that the preference of $AlPO_4$-17 for tetrahedral CH_4 molecules is higher than that for "capsular" CO in the adsorbed phase with separation factors being much higher at lower partial pressures of CH_4 in the gas phase.

Methane-Nitrogen/$AlPO_4$-17. $AlPO_4$-17 might be a promising adsorbent for the separation of CH_4-N_2 gas mixtures at 40°C and 101.3 kPa total pressure. Figure 13 shows that, according to the FH-VST predicted X-Y diagram, the separation would be efficient at low CH_4 partial pressures. As there is no CO in the system (the adsorbate which encounters most steric hindrance for adsorption in $AlPO_4$-17), FH-VST does not forecast azeotrope formation and selectivity reversal for this system. $AlPO_4$-17 is known to adsorb pure CH_4 in the largest amounts (compared to N_2 and CO) for pressures below 123 kPa.

Summary for $AlPO_4$-17. $AlPO_4$-17 could be considered a potential adsorbent for the reputably difficult separation of CH_4-N_2 gas mixtures. It could also be used for the separation of CH_4-CO mixtures at low CH_4 partial pressures.

4.2.3. $AlPO_4$-18.

Carbon Monoxide-Nitrogen/$AlPO_4$-18. Figure 14 illustrates the discrepancy in the predictions yielded by the three models. The a-ELM binary isotherm features a "hook" for the curve representing the N_2 and the

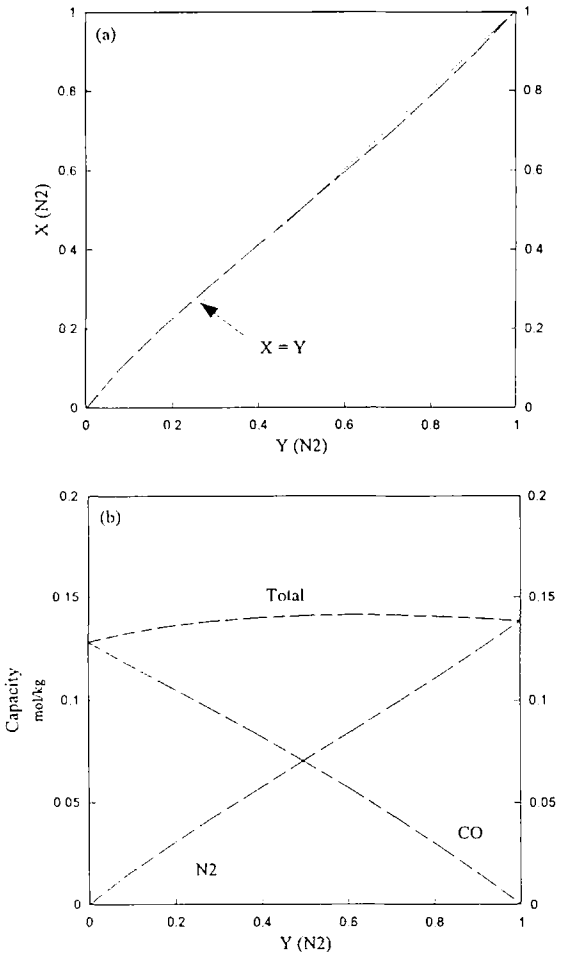

Figure 11. FH-VST predicted (a) X-Y diagram and (b) binary equilibrium isotherms for CO-N_2 adsorption in $AlPO_4$-17 at 40 C and 101.3 kPa total pressure.

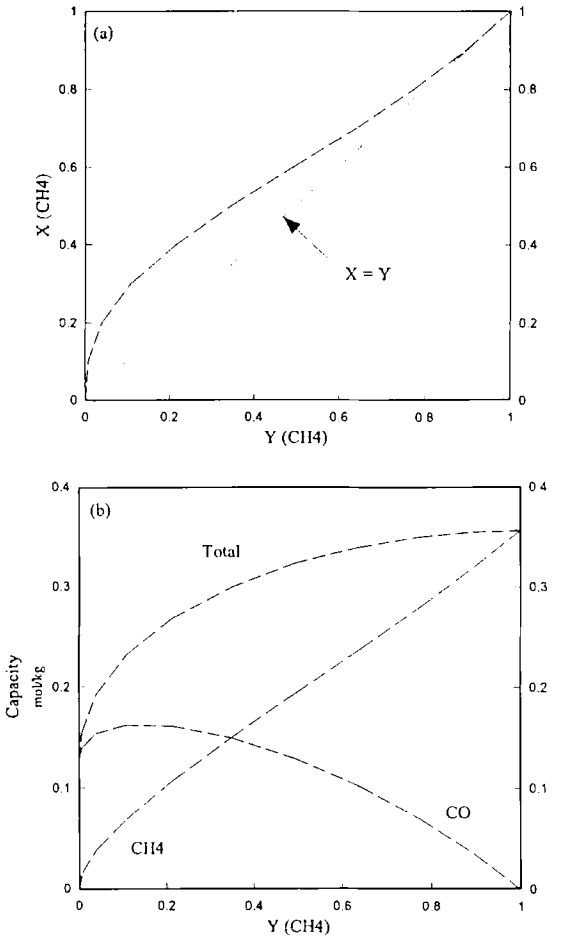

Figure 12. FH-VST predicted (a) X-Y diagram and (b) binary equilibrium isotherms for CO-CH_4 adsorption in $AlPO_4$-17 at 40 C and 101.3 kPa total pressure.

total amount adsorbed. IAST and d-ELM predict virtually linear binary isotherms with similar separation factors.

FH-VST predicts selectivity reversal which translates into a rounded curve for the total amount of mixture adsorbed, forming a positive deviation from ideality. This seems to enforce the idea that non-ideal behaviour such as azeotropy and selectivity reversal is very likely in small-pore aluminophosphate molecular sieves which feature similar capacities for the components of the binary gas mixture and considerable steric hindrance upon adsorption into the micropores.

The adsorption of a polar adsorbate can constitute both a benefit and a disadvantage for an energetically homogeneous aluminophosphate adsorbent. The dipole and quadrupole moments of CO molecules impart a certain degree of energetic heterogeneity to the adsorbent surface once they get adsorbed and become "part and parcel" of the adsorbent. Consequently, the benefit of CO adsorption in $AlPO_4$'s lies in the fact that the adsorbed CO molecules contribute self-potential to the total adsorption potential, a contribution much greater than that of adsorbed quadrupolar N_2 molecules. However, as the CO concentration increases in the adsorbed phase, the same electric moments of the CO molecules become responsible for more intense close-range repulsions, thus threatening the stability of the adsorbed phase (a drawback for the adsorption of polar gases). The energetically homogeneous adsorbent thereby faces a conflicting situation in which the tendency to retain the adsorbate which can

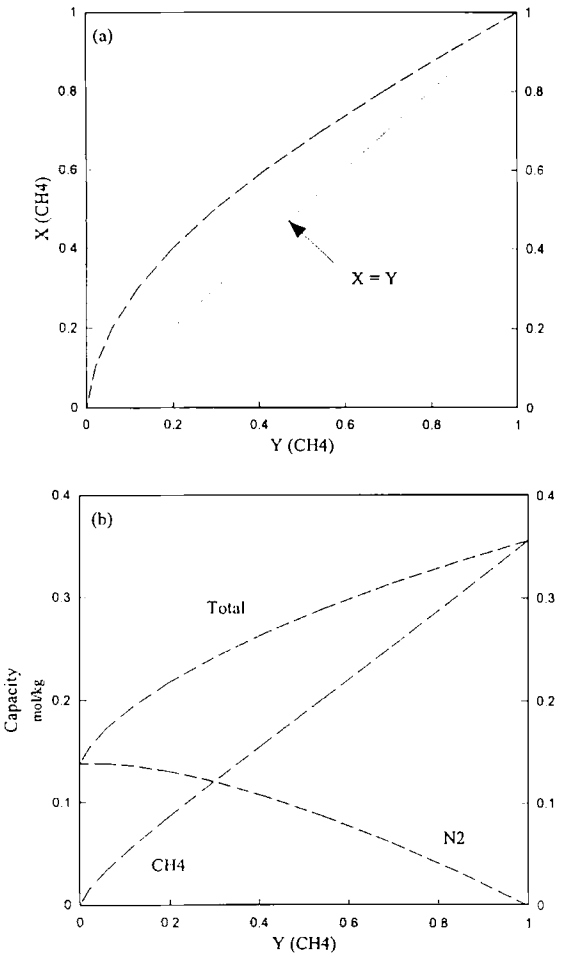

Figure 13. FH-VST predicted (a) X-Y diagram and (b) binary equilibrium isotherms for CH_4-N_2 adsorption in $AlPO_4$-17 at 40°C and 101.3 kPa total pressure.

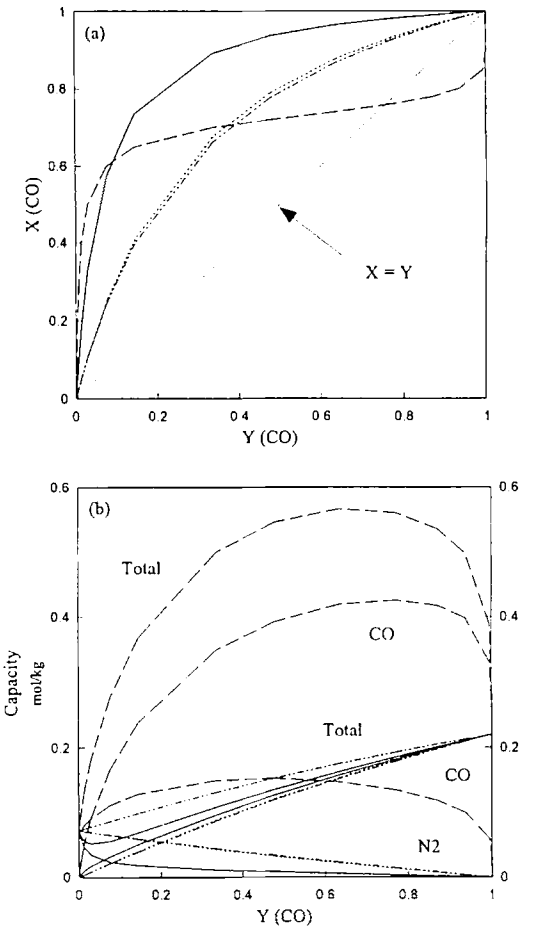

Figure 14. Predicted (a) X-Y diagram and (b) binary equilibrium isotherms for CO-N_2 adsorption in $AlPO_4$-18 at 40°C and 101.3 kPa total pressure: —— a-ELM, - - - - d-ELM, — - - IAST, and – – – FH-VST.

pay a large contribution in self-potential (CO) must oppose the tendency to ensure the stability of the adsorbed phase by restricting the access of the major self-potential contributor (CO).

Carbon Monoxide-Methane/$AlPO_4$-18. As illustrated by Fig. 15, the models predict virtually similar trends for the adsorption of this binary gas mixture as for the CO-N_2 gas mixture (Fig. 14), with CO expected to be the preferentially adsorbed species. The a-ELM "hook" for the curve representing the total amount adsorbed is less obvious. IAST and d-ELM predictions agree well for this system and are quite linear. FH-VST provides no surprise with its azeotrope and selectivity reversal prediction, and the rounded curve for the total amount adsorbed with positive deviations from ideality. The hypothesis regarding the relationship between non-ideal behaviour and steric hindrance can be again considered for this adsorption system.

Methane-Nitrogen/$AlPO_4$-18. Figure 16 shows that from the adsorption point of view this is a "normally-behaving" system in which CH_4 would be adsorbed in larger amounts. The selectivity values higher than 2 are predicted by these models with $AlPO_4$-18 for CH_4-N_2 mixtures (Table 8).

Summary for $AlPO_4$-18. Data on single-component equilibrium adsorption indicates that $AlPO_4$-18 has the highest capacity for CO, compared to the other two gases, at 101.3 kPa and 40°C, but it is not much higher than that for CH_4 at the same pressure and temperature (Fig. 4). IAST and d-ELM reflect this relative

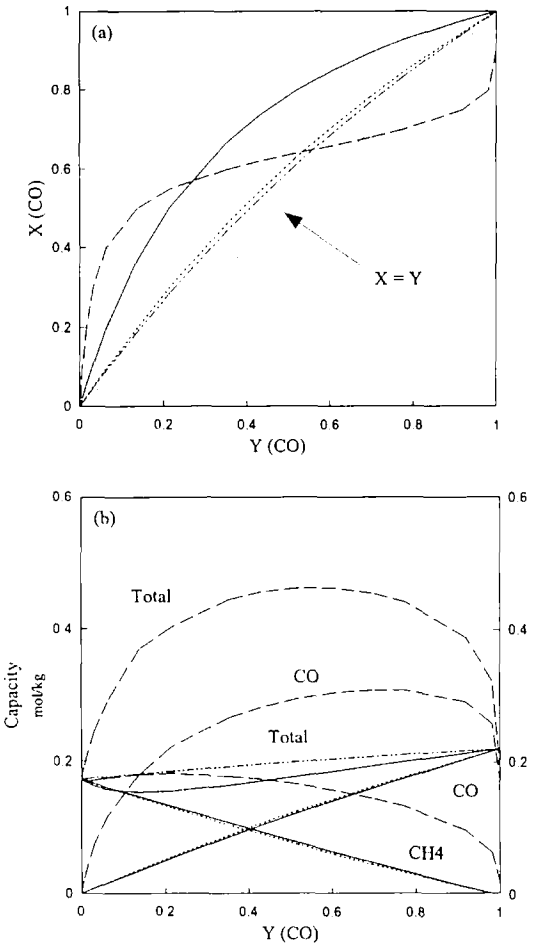

Figure 15. Predicted (a) X-Y diagram and (b) binary equilibrium isotherms for CO-CH_4 adsorption in $AlPO_4$-18 at 40 C and 101.3 kPa total pressure: —— a-ELM, - - - - d-ELM, – – IAST, and – – FH-VST.

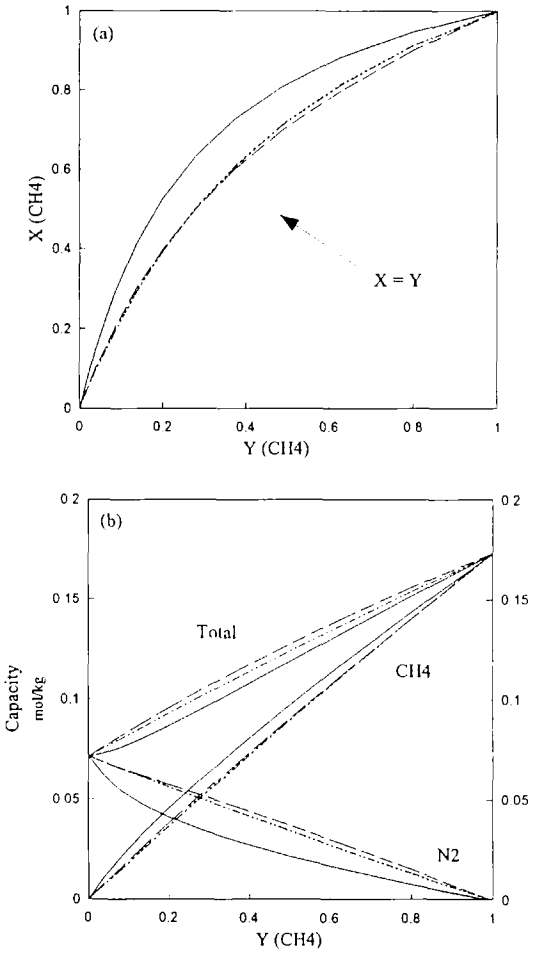

Figure 16. Predicted (a) X-Y diagram and (b) binary equilibrium isotherms for CH_4-N_2 adsorption in $AlPO_4$-18 at 40 C and 101.3 kPa total pressure: —— a-ELM, - - - - d-ELM, – – IAST, and – – FH-VST.

difference in pure-gas capacities by predicting easier separation if the relative ratio of the single-component capacities is high. Thus, the separation would be more successful for CO-N_2 gas mixtures than for CH_4-N_2 gas mixtures at 40°C and 101.3 kPa total pressure. The "odds" would be less favourable for the CO-CH_4 gas mixture because of the close values of the pure-gas adsorption capacities.

4.2.4. Summary for Binary Isotherm Predictions. The reliability of the information provided by the application of each of the three theories chosen (ELM, IAST, and the FH-VST for mixtures) depends on the accuracy of the pure gas adsorption isotherm fits. The greater the accuracy of the fits of the single-component adsorption isotherms, the higher the reliability of the binary gas mixture adsorption predictions. Collection of experimental binary adsorption data would be necessary for a final say on the predictive ability of each model. We are in the process of obtaining experimental binary isotherms for the systems studied in this work.

When the a-ELM equation is applied, the constant selectivity value characteristic to ELM is affected only by the ratio of the Langmuir constants (B_i/B_j) regressed from the respective pure-gas adsorption experimental isotherms. The influence of the Langmuir constants is obvious in the variation of the capacities of the adsorbent for the components and the mixture. When the d-ELM equation is applied, the constant selectivity value obtained is influenced by both the ratio of the Langmuir constants (B_i/B_j) and the ratio of the

monolayer volumes of the pure species (v_{mi}/v_{mj}). The effects of the Langmuir constants on the capacities of the adsorbents for the components and the mixture are tuned down by the effects of the monolayer volumes of each pure species. The investigation of the CO-N_2/$AlPO_4$-11 adsorption system at 23°C and 40°C shows that, as a result of the averaging of the monolayer volumes, when all the other models (IAST, FH-VST, d-ELM) predict equilibrium separation factors between 1 and 3, a-ELM predicts a value lower than 1 (indicating selectivity reversal), and should be considered questionable.

IAST predictions may be very sensitive to the difference in the spreading pressures of the two components, which can be very high if the adsorption capacities of the molecular sieve for the two components are widely different (e.g., mixtures of polar and non-polar or weakly polar gases, such as CO-N_2 and CO-CH_4). In addition, as Myers and Prausnitz (1965) emphasized, the accuracy of the fit in the low-pressure range is very important for reliable mixture predictions.

5. Conclusions

1. Physical adsorption is governed by steric effects in energetically homogeneous aluminophosphate molecular sieves.
2. In the pressure range investigated (<123 kPa), equilibrium adsorption capacities for CH_4 are the highest in $AlPO_4$-11 and $AlPO_4$-17, while CO is preferentially retained by $AlPO_4$-18. N_2 is adsorbed in relatively low amounts compared to the other two adsorbates in all the aluminophosphate molecular sieves investigated (except in $AlPO_4$-17).
3. Adsorption of CO in $AlPO_4$-17 and $AlPO_4$-18 and of CH_4 in $AlPO_4$-18 feature hysteresis which necessitates the incorporation of a thermal swing cycle when these adsorbents are used in pressure-swing adsorptive separation units.
4. For the pressure range investigated (<123 kPa), the Flory-Huggins form of the Vacancy Solution Theory (FH-VST) proves to be an excellent fitting tool for the pure-gas adsorption isotherms of N_2, CO, and CH_4 in aluminophosphate molecular sieves $AlPO_4$-11 and $AlPO_4$-18. Its fitting capabilities are slightly less satisfactory in the case of small-pore molecular sieve $AlPO_4$-17 in which steric effects are considerable when it comes to "capsular" adsorbate molecules such as N_2 and CO. These isotherms show slightly unfavourable S shape at low pressures.
5. The Langmuir equation also provides excellent fits for the pure N_2, CO, and CH_4 adsorption isotherms in $AlPO_4$-11 and $AlPO_4$-18. Its failure to fit the slightly unfavourable isotherm representing the adsorption of pure CO in $AlPO_4$-17, for which the Freundlich equation had to be used, indicates that it is not suitable for those systems in which adsorption is controlled by steric effects.
6. Prediction of binary mixture behaviour reveals that the energetically homogeneous aluminophosphate molecular sieves are more suitable for the separation of gas mixtures involving non-polar adsorbates (CH_4) and adsorbates with very small electric moments (N_2). According to model predictions, $AlPO_4$-11, $AlPO_4$-17, and $AlPO_4$-18 appear to have the potential to separate CH_4-N_2 mixtures.
7. FH-VST appears to predict an azeotrope and selectivity reversal in aluminophosphate systems whenever steric effects are considerable and the single-component equilibrium capacities are very similar. In the adsorption systems studied, most of the binary pairs containing CO as one of the components showed an azeotrope with small pore $AlPO_4$-17 and $AlPO_4$-18. These systems are expected to behave non-ideally.
8. The influence of adsorption temperature on binary mixture equilibrium in $AlPO_4$-11 is acknowledged by all models through a decrease in individual adsorption capacities and total amount adsorbed with an increase in temperature, as expected.

6. Future Work

This work will be continued by the determination of the experimental binary isotherms for the verification of the predicted binary isotherms.

Nomenclature

B, B_i, B_j	Langmuir constants	1/Pa
b_1	Henry's law constant	mol/kg Pa
T	atom capable of forming tetrahedra Si, Al, P	
k	Freundlich parameter	mol/kg Pa
n	Freundlich parameter dimensionless	
n_i	amount of species i adsorbed	mol/kg
n_i^0	amount of species i adsorbed at pressure P_i^0	mol/kg

$n_1^{\infty}, n_1^{\inf}$	limiting amount of adsorption	mol/kg
n_m	Langmuir monolayer capacity	mol/kg
P	pressure	Pa
P_i	partial pressure of species i	Pa
P_i^0	equilibrium pressure of pure component i at the same temperature and spreading pressure as the adsorbed mixture	Pa
R	universal gas constant	m^3 Pa/mol K
T	absolute temperature	K
v	volume of gas adsorbed	m^3
v_m	monolayer volume adsorbed	m^3
v_{mi}	monolayer volume of species i adsorbed	m^3
$v_{Mi}(=V_M)$	averaged monolayer volume	m^3
v_1	volume of gas adsorbed from a mixture	m^3
x_i	mole fraction of species i in the adsorbed phase	
y_i	mole fraction of species i in the gas phase	

Greek Letters

α_1	adsorbent polarizability cm^3
α_{12}	equilibrium adsorption separation factor (selectivity) dimensionless
α_{1v}	gas-vacancy interaction parameter dimensionless
π_i	spreading pressure of species i in the mixture Pa
θ	fractional coverage of the adsorbent surface dimensionless
θ_i	partial fractional coverage in multicomponent gas mixture adsorption dimensionless

Abbreviations

A11	molecular sieve $AlPO_4$-11
A17	molecular sieve $AlPO_4$-17
A18	molecular sieve $AlPO_4$-18
a-ELM	averaging-approach Extended Langmuir Model
d-ELM	direct-approach Extended Langmuir Model
IAST	Ideal Adsorbed Solution Theory
FH-VST	Flory-Huggins Vacancy Solution Theory

Acknowledgments

Financial support received from Natural Sciences and Engineering Research Council (NSERC) of Canada is gratefully acknowledged. $AlPO_4$ samples were kindly provided by Prof. Serge Kaliaguine of the Department of Chemical Engineering at Laval University.

References

Bennett, J.M., W.J. Dytrych, J.J. Pluth, J.W. Richardson, Jr., and J.V. Smith, "Structural Features of Aluminophosphate Materials with Al/P = 1," *Zeolites*, **6**, 349–359 (1986).

Breck, D.W., *Zeolite Molecular Sieves: Structure, Chemistry and Use*, John Wiley & Sons, New York, Inc., 1974.

Broughton, D.B., "Adsorption Isotherms for Binary Gas Mixtures," *Ind. Eng. Chem.*, **40**(8), 1506–1508 (1948).

Cochran, T.W., R.L. Kabel, and R.P. Danner, "Vacancy Solution Theory of Adsorption Using Flory-Huggins Activity Coefficient Equations," *AIChE Journal*, **31**(2), 268–277 (1985).

Graham, D., "Adsorption Equilibria" in *Adsorption, Ion Exchange and Dialysis*, AIChE Chemical Engineering Progress Symposium Series, **55**(24), 17–23 (1959).

Grillet, Y., P.L. Llewellyn, H. Reichert, J.P. Coulomb, N. Pellenq, and J. Rouquerol, "Confinement in Micropores and Enthalpies of Physisorption," in *Characterization of Porous Solids III*, J. Rouquerol et al. (Eds.), Studies in Surface Science and Catalysis, Elsevier, Amsterdam, Vol. 87, pp. 525–534, 1994.

Innes, W.B. and H.H. Rowley, "Adsorption Isotherms of Mixed Vapors of Carbon Tetrachloride and Methanol on Activated Charcoal at 25°C," *J. Phys. Coll. Chem.*, **51**, 1154–1171 (1947).

Innes, W.B., R.B. Olney, and H.H. Rowley, "Adsorption Isotherms of Mixed Vapors of Benzene and Methanol on Activated Charcoal at 25°C," *J. Phys. Coll. Chem.*, **55**, 1324–1334 (1951).

Kemball, C., E.C. Rideal, and E.A. Guggenheim, "Thermodynamics of Monolayers," *Trans. Faraday Soc.*, **44**, 948–954 (1948).

Langmuir, I., "Adsorption of Gases on Plane Surfaces of Glass, Mica and Platinum," *J. Am. Chem. Soc.*, **40**, 1361–1403 (1918).

Lillerud, K.P. and D. Akporiaye, "Systematic Relationships Between the Structures of CHA, AEI and KFI," in *Zeolites and Related Microporous Materials: State of the Art 1994*, J. Weitkamp et al. (Eds.), *Studies in Surface Science and Catalysis*, Elsevier, Amsterdam, Vol. 84, pp. 543–550 (1994).

Markham, E.C. and A.F. Benton, "The Adsorption of Gas Mixtures by Silica," *J. Am. Chem. Soc.*, **53**, 497–507 (1931).

Martens, J.A. and P.A. Jacobs, "Crystalline Microporous Phosphates: a Family of Versatile Catalysts and Adsorbents," in *Advanced Zeolite Science and Applications, Studies in Surface Science and Catalysis*, Elsevier, Amsterdam, Vol. 85, pp. 653–685, 1994.

Meier, W.M. and D.H. Olson, *Atlas of Zeolite Structure Types*, 3rd. rev. ed., Butterworth-Heinemann, London, 1992.

Myers, A.L. and J.M. Prausnitz, "Thermodynamics of Mixed-Gas Adsorption," *A.I.Ch.E.J.*, **11** (1), 121–127 (1965).

Rudolf, P.R. and C.E. Crowder, "Structure Refinement and Water Location in the Very Large-Pore Molecular Sieve VPI-5 by X-ray Rietveld Techniques," *Zeolites*, **10**, 163 (1990).

Ruthven, D.M., *Principles of Adsorption and Adsorption Processes*, John Wiley & Sons, New York, 1984.

Simmen, A., L.B. McCusker, Ch. Baerlocher, and W.M. Meier, "The Structure Determination and Rietveld Refinement of the Aluminophosphate $AlPO_4$-18," *Zeolites*, **11**, 654–661 (1991).

Stelmack, P., "Adsorption of N_2, CO, CH_4, and Binary Mixtures of these Gases in Zeolite 5A, Clinoptilolite, and $AlPO_4$-11 Molecular Sieves," B.A.Sc. Thesis, University of Ottawa, Ottawa, 1994.

Suzuki, M., *Adsorption Engineering*, Kodansha Ltd., Tokyo, and Elsevier Science Publishers B.V., Amsterdam, 1990.

Szostak, R., *Handbook of Molecular Sieves*, Van Nostrand Reinhold, New York, 1992.

Theocharis, C.R. and M.R. Gelsthorpe, "Modified Aluminophosphate Microporous Solids," in *Characterization of Porous Solids*, K.K. Unger et al. (Eds.), Elsevier Science Publishers B.V., Amsterdam, 1988.

Valenzuela, D.P. and A.L. Myers, *Adsorption Equilibrium Data Handbook, Prentice-Hall Advanced Reference Series*, Prentice-Hall, Englewood Cliffs, New Jersey, 1989.

Wilson, S.T., "Synthesis of $AlPO_4$-Based Molecular Sieves," in *Introduction to Zeolite Science and Practice, Studies in Surface Science and Catalysis*, H. van Bekkum, E.M. Flanigen, and J.C. Hansen (Eds.), Elsevier, Amsterdam, Vol. 58, pp. 137–151, 1991.

Yang, R.T., *Gas Separation by Adsorption Processes*, Butterworth Publishers, Mass. U.S.A., 1987.

Zeldowitsh, J., "On the Theory of the Freundlich Adsorption Isotherm," *Acta Physicochim*, U.R.S.S., **1**(6), 961–973 (1935).